

THE CONTRAST SOURCE-EXTENDED BORN MODEL FOR 2D SUBSURFACE SCATTERING PROBLEMS

L. Crocco

CNR-IREA, National Research Council
Institute for the Electromagnetic Sensing of the Environment
Via Diocleziano 328, Napoli I-80124, Italy

M. D'Urso

Giugliano Research Center — Integrated System Analysis
SELEX Sistemi Integrati
Via Cicumvallazione Esterna di Napoli, Zona ASI
Giugliano, Napoli I-80014, Italy

T. Isernia

DIMET — Dipartimento di Informatica, Matematica, Elettronica e
Trasporti
Mediterranea University of Reggio Calabria
Via Graziella, Loc. Feo di Vito, Reggio, Calabria I-89100, Italy

Abstract—In this paper, we describe a new full-wave integral equation model to tackle electromagnetic scattering problems arising from objects buried in layered media. Such a model is a rewriting of the usually adopted Contrast Source integral equation and is named Contrast Source-Extended Born (CS-EB) owing to this circumstance and to the relationship existing among its linearization and the Extended Born approximation. By means of this alternative formulation, it is possible to modify the relationship among the scatterer permittivity and the field it scatters, thus possibly reducing the degree of non-linearity of this latter relationship. Accordingly, in these cases, the adoption of the CS-EB model may be convenient with respect to traditional ones in both forward and inverse scattering problems.

1. INTRODUCTION

In many geoscience applications, ranging from near surface geophysics explorations to underwater reservoir detection and demining, the development of approaches to achieve fast and accurate solutions of forward and inverse electromagnetic scattering problems by lossy dielectric objects buried in a lossy medium is of great interest.

In this framework, integral equation formalism [1] is widely used to model the scattering phenomenon. As far as the forward problem is concerned, the relevant integral equation is typically solved in a discretized fashion via method of moments and involves a dense linear system [2]. To avoid direct matrix inversion, the system is iteratively solved by means of conjugate-gradient fast Fourier transform (CG-FFT) algorithms [3]. However, the efficiency of CG-FFT depends on the condition number of the original linear system, so that it can still be computationally demanding. Hence, approximate solutions, such as the Extended Born (EB) approximation [4] and its heuristic extensions [5] or algebraic preconditioners [6, 7] are worth studying as means to improve the convergence rate. The inverse scattering problem is non-linear and ill-posed [8] and it is usually cast as the global optimization of a suitable cost functional [9–15].

In this case, the difficulties that arise are not merely computational. As matter of fact, the optimization task cannot be tackled through global approaches, whose computational cost is not affordable due to the large number of unknown parameters, and local optimization methods are usually exploited. However, due to the nonlinear relationship amongst the data and the unknowns, these latter may lead to “false” solutions deeply different from the ground truth [16], so that it is necessary to understand how to reduce the occurrence of these false solutions (for instance by means of suitable a priori information or proper regularization).

With respect to the case of objects embedded in an unbounded homogeneous medium, an alternative full wave integral equation model has been recently introduced to overcome, or at least reduce, the aforementioned issues by taking advantage of the features of the Green's function [17–19]. This new formulation is named Contrast Source-Extended Born (CS-EB) model owing to two circumstances:

- i the integral equation underlying the model is a non-approximated rewriting of the Contrast Source (CS) equation [20];
- ii the linearization of this equation corresponds, for homogeneous scatterers, to the EB approximation [4].

In particular, the CS-EB model can provide a convenient choice for the forward problem, since its solution via series iterations is either

more widely applicable or faster convergent than the traditional Born series [17, 19]. Moreover, in the inverse problem, it can reduce the *degree of nonlinearity* [21] of the relationship between the parameters embedding the dielectric characteristics and the scattered field as compared to the CS model, thus reducing possible occurrence of false solutions [22–24].

Recently, a rigorous comparison between the two models has been carried out [25], allowing to give criteria to select the most suitable one to be exploited depending on the scenario and the targets at hand. For instance, such an analysis has shown that when a sufficient amount of loss is present in the embedding medium, the CS-EB model is the most convenient choice to handle scattering problems. Conversely, for lossless backgrounds and negative contrasts the CS model is more appropriate.

In subsurface scattering problems, losses are usually present within the embedding medium and/or the targets, so that it is worth considering the CS-EB model also in this context. On the other hand, owing to the different expression of the underlying Green function with respect to the homogeneous background case, the adoption of the model as previously formulated is not possible. Accordingly, in this paper we derive a CS-EB formulation for the scattering from dielectric objects buried in a lossy half-space. With respect to this new CS-EB formulation, we then introduce the corresponding series expansion to solve the forward problem and provide tools to foresee its applicability and improve its convergence by means of the generalized *overrelaxation* method [26]. Also, we recall how the obtained CS-EB model can be exploited in the inverse problem by suitably adapting previously developed strategies. Note that while we will consider the 2D scalar case, the achieved model can be readily generalized to the 3D case following the reasonings in [18, 19].

The paper is organized as follows. Section 2 is devoted to the formulation of the CS-EB model for the half-space problem. In Section 3, we discuss the features of the model. In Section 4, the CS-EB series is introduced and discussed and a numerical example is given to show how it can outperform the Born series. Section 5 describes the CS-EB inversion strategy and provide a numerical example. Conclusions follow.

Throughout the paper the time-harmonic factor $\exp(j\omega t)$ is assumed and dropped.

2. CS-EB FORMULATION FOR THE HALF-SPACE GEOMETRY

The geometry of the scattering problem is shown in Fig. 1. The scenario is constituted of two half-spaces separated by a planar interface parallel to the x -axis. The upper half space is air, while the lower one is soil. One or more targets are buried in the soil, within the search domain D , whose center is at a distance h from the interface. The data are collected under a multistatic/multiview configuration by exploiting N_T time-harmonic TM-polarized line sources located along a rectilinear domain Γ_T at a distance y_T from the interface and N_R elementary probes displaced along the rectilinear domain Γ_R at distance y_R . All media are assumed to be linear, isotropic and non-magnetic and described by their frequency-independent relative permittivities ϵ_i and conductivities σ_i (S/m), $i = 1, 2, D$; ϵ_D and σ_D are allowed to change with the position $\underline{r} = (x, y)$ within D . The magnetic permeability is everywhere equal to that of free space, μ_0 (H/m). The complex equivalent permittivity of each medium is defined as $\tilde{\epsilon}_i = \epsilon_i - j\sigma_i/(\omega\epsilon_0)$, ϵ_0 being the permittivity of free space, ω the angular frequency and $j = \sqrt{-1}$.

Electromagnetic scattering problems are usually cast through the CS integral equation model [20], which reads:

$$E_s(\underline{r}) = \int_D g_{21}(\underline{r}, \underline{r}') J(\underline{r}') d\underline{r}' = \mathbf{G}_{21} J \quad \underline{r} \in \Gamma_R, \quad (1)$$

$$\begin{aligned} J &= \chi(\underline{r}) E_{\text{inc}}(\underline{r}) + \chi(\underline{r}) \int_D g_{22}(\underline{r}, \underline{r}') J(\underline{r}') d\underline{r}' \\ &= \chi(\underline{r}) E_{\text{inc}}(\underline{r}) + \mathbf{G}_{22} J \quad \underline{r} \in D. \end{aligned} \quad (2)$$

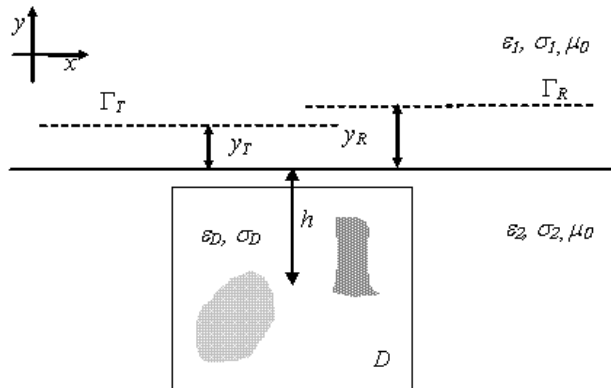


Figure 1. Geometry of the problem.

In (1) and (2), E_s is the scattered field observed in the upper medium on Γ_R , E_{inc} is the incident field in D , $\chi(\underline{r}) = \tilde{\epsilon}_D(\underline{r})/\tilde{\epsilon}_2 - 1$ is the *contrast* amongst the (complex) equivalent permittivities of the targets and the background and $J = \chi E$ is the contrast source, E being the total field induced inside the investigated region D . \mathbf{G}_{21} , \mathbf{G}_{22} denote the radiation operators which relate the induced currents in D to the scattered field on Γ_R and inside D , respectively.

For the scenario at hand, the Sommerfield-Green's functions g_{21} and g_{22} are expressed in terms of spectral integrals [1]. In particular, g_{22} is given as the sum of two contributions, the first one coincides with the Green's function of a *homogeneous* background

$$g_{22}^H(\underline{r}, \underline{r}') = -\frac{jk_2^2}{4} H_0^{(2)}(k_2|\underline{r} - \underline{r}'|), \tag{3}$$

where $\underline{r}' = (x', y')$, $k_2 = \omega\sqrt{\tilde{\epsilon}_2\mu_0}$, $H_0^{(2)}$ is the Hankel function of zero order and second kind. The second contribution takes into account the presence of the interface between the two half-spaces:

$$g_{22}^I(\underline{r}, \underline{r}') = -\frac{ik_2^2}{4\pi} \int_{-\infty}^{\infty} \frac{\beta_2 - \beta_1}{\beta_2 + \beta_1} \times \exp [i\beta_2 (y + y')] \exp [-i\kappa (x - x')] \frac{1}{\beta_2} d\kappa. \tag{4}$$

where $\beta_i = \sqrt{\omega^2\tilde{\epsilon}_i\mu_0 - \kappa^2}$, $i = 1, 2$ and $\text{Im}[\beta_i] \leq 0$.

By using the above expressions, one can rewrite Eq. (2) as:

$$J(\underline{r}) = \chi(\underline{r})E_{inc}(\underline{r}) + \chi(\underline{r})\mathbf{G}_{22}^H J + \chi(\underline{r})\mathbf{G}_{22}^I J \tag{5}$$

wherein

$$\mathbf{G}_{22}^H J = \int_D g_{22}^H(\underline{r}, \underline{r}') J(\underline{r}') d\underline{r}' \tag{6}$$

and

$$\mathbf{G}_{22}^I J = \int_D g_{22}^I(\underline{r}, \underline{r}') J(\underline{r}') d\underline{r}'. \tag{7}$$

To achieve the CS-EB formulation we are pursuing, let us add and subtract the contrast source $J(\underline{r})$ into the argument of the *homogeneous* integral operator (6),

$$\begin{aligned} \mathbf{G}_{22}^H J &= \int_D g_{22}^H(\underline{r}, \underline{r}') [J(\underline{r}') + J(\underline{r}) - J(\underline{r})] d\underline{r}' = J(\underline{r}) \int_D g_{22}^H(\underline{r}, \underline{r}') d\underline{r}' \\ &+ \int_D g_{22}^H(\underline{r}, \underline{r}') [J(\underline{r}') - J(\underline{r})] d\underline{r}' = \mathbf{I}f_D J + \mathbf{\Delta}\mathbf{G}_{22}^H J, \end{aligned} \tag{8}$$

where \mathbf{I} denotes the identity operator. By doing so, we have split $\mathbf{G}_{22}^{\mathbf{H}}$ into two terms, the first one being a point-to-point relationship for the contrast source. Notably, this term dominates the second one as long as losses are present in the background medium. As a matter of fact, the exponential decay of $g_{22}^{\mathbf{H}}$ (increasingly fast with losses) makes $\Delta\mathbf{G}_{22}^{\mathbf{H}}J$ negligible when $\underline{r} \neq \underline{r}'$, while, for $\underline{r} = \underline{r}'$, $\Delta\mathbf{G}_{22}^{\mathbf{H}}$ is null, being its argument equal to zero.

By substituting Eq. (8) into Eq. (2) and grouping the terms in the contrast source, one gets, after some manipulations, the new integral equation:

$$J(\underline{r}) = \xi(\underline{r})E_{\text{inc}}(\underline{r}) + \xi(\underline{r})\mathbf{G}_{22}^{\text{MOD}}J \quad \underline{r} \in D, \quad (9)$$

where

$$\mathbf{G}_{22}^{\text{MOD}}J = \mathbf{G}_{22}^{\mathbf{I}}J + \Delta\mathbf{G}_{22}^{\mathbf{H}}J, \quad (10)$$

$$\xi(\underline{r}) = \chi(\underline{r})[1 - \chi(\underline{r})f_D(\underline{r})]^{-1}. \quad (11)$$

Equation (9) is equivalent and formally analogous to the CS Eq. (2), so that we can use it, together with Eq. (1), as an alternative way to formulate the scattering problem at hand. In the so obtained CS-EB model, the *modified radiation operator* $\mathbf{G}_{22}^{\text{MOD}}$ replaces \mathbf{G}_{22} , while the electromagnetic parameters of the scatterers are embedded into the *modified contrast function* ξ rather than in χ . As we will discuss in the next section, the adoption of these quantities allows some interesting outcomes when solving scattering problems.

Let us explicitly note that the obtained equation is different from the one that defines the CS-EB model in the homogeneous case, wherein the modified radiation operator coincides with $\Delta\mathbf{G}_{22}^{\mathbf{H}}$ [17]. Conversely, the expression of the modified contrast ξ is unchanged, since this latter has been herein defined in such a way that it is independent from the depth at which the target is buried.

3. FEATURES OF THE CS-EB MODEL

The result obtained in the previous Section only descends from simple algebraic passages, so that it is reasonable to ask what advantages (if any) can be drawn from it.

A first interesting observation holds whenever the second term at the right hand side of (9) is negligible, i.e., when $J(\underline{r}) \approx \xi(\underline{r})E_{\text{inc}}(\underline{r})$. As a matter of fact, it is easy to verify that, for homogeneous targets, this approximation for the contrast source coincides with the result of the Extended Born approximation [4]. This circumstance tells us that the CS-EB zero-th order approximation has an *extended* validity with respect to the Born approximation, that is, the zero-th order

approximation for the CS model. Accordingly, a number of cases exists in which the linearization of the CS-EB equation provides a better estimate of the contrast source with respect to CS equation [25].

In more general cases, where a linearized approximation may be not sufficient to properly model the scattering problem, the question arises of understanding the possible convenience of the proposed model. As long as the effect of the interface on the contrast source can be neglected (as for instance for deeply buried targets or highly lossy environments), $\mathbf{G}_{22}^{\text{MOD}} \approx \Delta \mathbf{G}_{22}^{\text{H}}$ and the formulation coincides with that of the homogeneous case. Therefore, we can exploit our previous results to assess the effectiveness of the CS-EB model [17–19, 22] as well as of the analytical tools provided in [25] to foresee if and when the CS-EB model will be a more convenient choice with respect to the CS one.

When the effect of the interface cannot be neglected, let us consider the formal inversion of Eq. (9), which reads:

$$J(r) = [\mathbf{I} - \xi \mathbf{G}_{22}^{\text{MOD}}]^{-1} \xi(r) E_{\text{inc}}(r). \quad (12)$$

By substituting this expression into the *data* equation (1), one gets an explicit relationship amongst the scattered field E_s and the modified contrast function $\xi(r)$:

$$E_s(r) = \mathbf{G}_{21} [\mathbf{I} - \xi \mathbf{G}_{22}^{\text{MOD}}]^{-1} \xi(r) E_{\text{inc}}(r). \quad (13)$$

The nonlinearity of the above relationship is ruled by the L^2 norm over D of the operator $\xi \mathbf{G}_{22}^{\text{MOD}}$, $\|\xi \mathbf{G}_{22}^{\text{MOD}}\|$, which indeed represents the *degree of nonlinearity* (DNL) of the scattering model [21]. As a matter of fact:

- if $\|\xi \mathbf{G}_{22}^{\text{MOD}}\| \ll 1$, $J \approx \xi E_{\text{inc}}$ and (13) is a linear relationship;
- if $\|\xi \mathbf{G}_{22}^{\text{MOD}}\| < 1$, the inverse operator in (12) can be expanded into a Neumann series, whose truncation corresponds to a polynomial relationship ruled by $\|\xi \mathbf{G}_{22}^{\text{MOD}}\|$;
- if $\|\xi \mathbf{G}_{22}^{\text{MOD}}\| > 1$ the relationship is non-polynomial.

The DNL provides an explicit way to appraise the convenience and limitations of an integral equation model with respect to the solution of both the forward and the inverse problem. As a matter of fact, an increasing value of the DNL corresponds to an increase of multiple scattering interactions that slow down the convergence of iterative forward solvers and increase occurrence of local minima in the inverse one [17, 21, 25].

From the formal equivalence between the CS-EB model and the CS one, it follows that the DNL for the CS is given by the norm $\|\chi \mathbf{G}_{22}\|$.

Hence, the comparison of the two DNLs gives a direct way to compare the models. To this end, we consider in the following the upper bounds obtained from the application of the Schwartz inequality, i.e.,:

$$\begin{aligned} \|\xi \mathbf{G}_{22}^{\text{MOD}}\| &\leq \|\xi\| \|\mathbf{G}_{22}^{\text{MOD}}\|, \\ \|\chi \mathbf{G}_{22}\| &\leq \|\chi\| \|\mathbf{G}_{22}\|. \end{aligned} \quad (14)$$

Although these bounds do not give an exact quantification of the DNLs, they are very convenient for our purposes, as they allow us to separately discuss the effect of the targets features (embedded in ξ and χ) from those of the scenario under test contained in the radiation operators.

As far as the effect of the scenario is concerned, observing that

$$\begin{aligned} \|\mathbf{G}_{22}^{\text{MOD}}\| &\leq \|\mathbf{G}_{22}^{\text{I}}\| + \|\Delta \mathbf{G}_{22}^{\text{H}}\| \\ \|\mathbf{G}_{22}\| &\leq \|\mathbf{G}_{22}^{\text{I}}\| + \|\mathbf{G}_{22}^{\text{H}}\|, \end{aligned} \quad (15)$$

one notices that the comparison essentially depends on the norms of the homogeneous terms. These latter, as shown by the plots given in [17, 23, 25] are comparable in most cases, so that the two models can be considered as equivalent with respect to this factor.

Some interesting differences arise when considering the first factor. As a matter of fact, from the definition of ξ given in Eq. (11), it descends that if

$$\|1 - \chi(r)f_D(r)\| > 1, \quad (16)$$

then $\|\xi\| < \|\chi\|$, so that the DNL of the CS-EB is lower than the CS one. Conversely, when condition (16) is not fulfilled, the CS is expected to be the more convenient model to exploit. In particular, given the definition of $\|\xi\|$, which only depends on the homogeneous term of the Green's function, we can again take advantage of previous results [17, 25] to address the choice.

Another observation can be done concerning the DNL of the CS-EB model. In the model's derivation, the integration domain appearing in the function f_D coincides with the scattering region D . Such a choice is not necessary. As a matter of fact, the choice of the integration domain is a degree of freedom for the CS-EB model, as it does not change the model's features, provided the auxiliary function ξ is defined consistently. As a consequence of this, a proper choice of the integration domain in f_D can modify the DNL of the model [23]. According to this observation, in the following we replace f_D with f_Ω to remark that the integration domain Ω can be either equal to D or chosen in such a way to optimize the model's performances.

4. USING THE CS-EB MODEL IN THE FORWARD PROBLEM

4.1. CS-EB Series: Applicability and Rate of Convergence

As discussed in the previous Section, as long as $\|\xi \mathbf{G}_{22}^{\text{MOD}}\| < 1$, the inverse operator in (12) can be expanded into a Neumann series [27], whose structure is the same as the usual Born series, as:

$$J(r) = \sum_{n=0}^{+\infty} (\xi \mathbf{G}_{22}^{\text{MOD}})^n \xi(r) E_{\text{inc}}(r). \quad (17)$$

From a numerical point of view, the evaluation of such a series is straightforward. As a matter of fact, by recalling the definition of power of a linear operator [27], the contrast source solution can be efficiently built using the iterative scheme

$$J^{(k+1)} = J^{(0)} + \xi \mathbf{G}_{22}^{\text{MOD}} J^{(k)} \quad k \geq 0, \quad (18)$$

where $J^{(0)}$ is the CS-EB approximation and the operator $\mathbf{G}_{22}^{\text{MOD}}$ is evaluated using FFT codes. As a matter of fact, by exploiting Eq. (8) in Eq. (10) one can rewrite this operator as:

$$\mathbf{G}_{22}^{\text{MOD}} J = \mathbf{G}_{22} J - \mathbf{I} f_{\Omega} J, \quad (19)$$

wherein the integral f_{Ω} is computed via FFT as the convolution product between a function that assumes unitary value in Ω (and it is zero elsewhere) and the homogeneous Green's function, while the radiation operator \mathbf{G}_{22} is computed via FFT as usual.

Although (17) and (18) represent a simple way to solve the problem, their practical usefulness is limited, unless a criterion is available to assess the convergence. To this aim, it proves again convenient to exploit the upper bound (14), as it provides a sufficient condition to check the applicability of the new series (17), as well as to achieve information on its rate of convergence. In particular, results observed in the homogeneous case [17, 19] and a large number of numerical simulations has suggested that an empirical condition that has to be fulfilled to foresee the converge of the series is:

$$\|\xi\| \|\mathbf{G}_{22}^{\text{MOD}}\| \leq 2. \quad (20)$$

In order to check this condition, one has to appraise the two factors. As far as $\xi(r)$ is concerned, given the characteristics of the scatterer at hand, this norm is easily computed by recalling that any scalar function is equivalent to a diagonal operator whose diagonal is given by the values of the function (in this case the values of ξ for

$r \in D$). Thus, by applying the definition of the norm of a diagonal operator [27], one gets:

$$\|\xi\| = \max_{r \in D} (|\xi(r)|). \quad (21)$$

Note again that a proper choice of the integration domain Ω in f_Ω allows to act on the value of (21).

As far as the norm of the modified radiation operator is concerned, this latter is defined as

$$\|\mathbf{G}_{22}^{\text{MOD}}\| = \lambda_1, \quad (22)$$

λ_1 being the leading singular value [27]. Hence, this norm can be obtained by applying standard numerical routines to the matrix arising from the proper discretization of the operator $\mathbf{G}_{22}^{\text{MOD}}$.

As the properties of such an operator do not depend on the scatterers but only on the geometric and electromagnetic characteristics of the investigated domain, it is possible to build some *universal plots* which completely describe the $\|\mathbf{G}_{22}^{\text{MOD}}\|$ as a function of those quantities. Some cuts of this diagram are shown in Fig. 2 wherein the behavior of the norms $\|\mathbf{G}_{22}^{\text{I}}\|$ and $\|\Delta\mathbf{G}_{22}^{\text{H}}\|$ are also reported for the sake of comparison. In Fig. 2(a) the dependence on the background tangent loss is given, for a fixed dimension of the square scattering region at hand (L is the side of D) and for a fixed depth, h . As it can be observed $\|\mathbf{G}_{22}^{\text{MOD}}\|$ decreases for increasing losses, moreover,

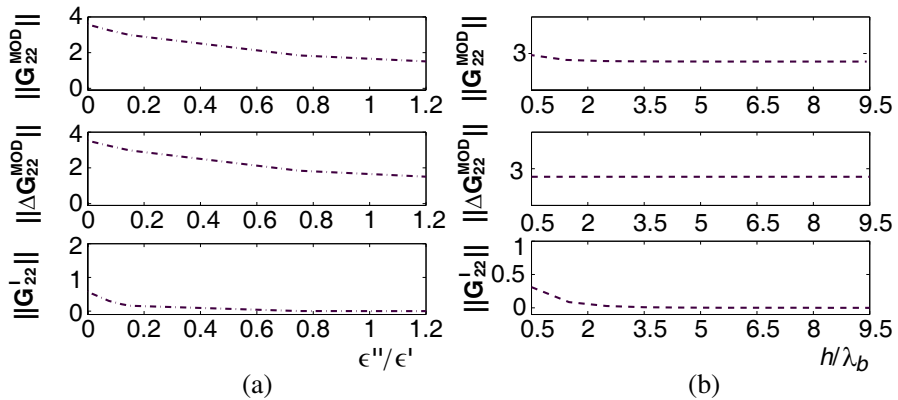


Figure 2. Behavior of $\|\mathbf{G}_{22}^{\text{MOD}}\|$, $\|\Delta\mathbf{G}_{22}^{\text{H}}\|$ and $\|\mathbf{G}_{22}^{\text{I}}\|$ versus the tangent loss in the background medium (a), for $L/\lambda_b = 1.0$ and $h/\lambda_b = 1.5$, λ_b being the wavelength in the host medium, and versus the depth h/λ_b of the scattering domain (b), for $L/\lambda_b = 1.0$ and $\epsilon''/\epsilon' = 0.15$.

its behavior is almost completely dominated by the homogeneous term $\Delta \mathbf{G}_{22}^H$. Conversely, when considering a fixed amount of loss in the background and a fixed depth of the region D , the norms grow with L . However, also in this case, the contribution of the inhomogeneous term is one order of magnitude lower. Finally, for a fixed dimension of the scattering domain and a fixed value of the tangent loss, $\|\mathbf{G}_{22}^{\text{MOD}}\|$ exhibits a decrease with depth (see Fig. 2(b)) which is of course due to the inhomogeneous term becoming more and more negligible when the region under test moves apart from the interface. Note that, different from the homogeneous case [17], it is not possible to introduce a single universal plot for the behavior of $\|\mathbf{G}_{22}^{\text{MOD}}\|$, due to the presence of the inhomogeneous part \mathbf{G}_{22}^I in the operator. On the other hand, the inspection of the universal plot for a given depth allows one to a priori understand whether the inhomogeneous scenario at hand can be conveniently simplified into a homogeneous one, regardless of the embedded scatterer. Of course, this brings benefits in terms of computational burden and complexity as the evaluation of the spectral integrals required to compute the Green's function would be avoided.

4.2. Enhancing the CS-EB Series Using the Generalized Over-relaxation Method

The introduced universal plots and Eq. (21) allow to obtain a priori information on the applicability and rate of convergence of the proposed series (the lower $\|\xi \mathbf{G}_{22}^{\text{MOD}}\|$, the faster the convergence). As a matter of fact, for a given scatterer and a fixed scenario, one can use them to check if condition (20) is matched. Hence, they provide a practical way to appraise if the solution of the forward problem via the simple series iterations (18) is possible or not. It is however worth remarking that, in case the series is not applicable, the introduced CS-EB model can be exploited in the framework of a traditional CG-FFT which is expected to reach convergence faster than CS based schemes, as long as $\|\xi \mathbf{G}_{22}^{\text{MOD}}\| \leq \|\chi \mathbf{G}_{22}\|$.

As a further alternative to extend the applicability of the CS-EB series, it is possible to devise a modified series solution based on a generalized overrelaxation method [20]. Such a method consists in deriving a Neumann series from a modified version of the relevant integral equation achieved through the introduction of a relaxation parameter.

In particular, by exploiting such a procedure, the iterative process (18) is replaced by

$$J^{(k+1)} = J^{(0)} + \mathbf{L}_\alpha J^{(k)} \quad k \geq 0, \quad (23)$$

where the operator \mathbf{L}_α is defined as $\mathbf{L}_\alpha = (1 - \alpha)\mathbf{I} + \alpha\xi\mathbf{G}_{22}^{\text{MOD}}$ and the relaxation parameter α is such that the residual at the first iteration is minimized and it is expressed as:

$$\alpha = \frac{[\xi\mathbf{G}_{22}^{\text{MOD}}J^{(0)}] \mathbf{L}_\alpha [\xi\mathbf{G}_{22}^{\text{MOD}}J^{(0)}]^*}{\|\mathbf{L}_\alpha [\xi\mathbf{G}_{22}^{\text{MOD}}J^{(0)}]\|^2}. \quad (24)$$

Interestingly, while only requiring the low computational overhead needed to evaluate the parameter (24), the modified series (23) has an increased range of convergence with respect to the previous one, so that it makes possible to solve in a larger number of cases the forward problem via simple iterations [20].

4.3. Numerical Examples

Let us consider a homogeneous square target of side 0.6 m, of permittivity $\epsilon = 10$ and conductivity $\sigma = 5 \times 10^{-3}$ S/m, buried in a lossy soil ($\epsilon_2 = 4$, $\sigma_2 = 10^{-2}$ S/m). The center of the target is buried at a depth of 0.4 m from the interface and the working frequency is 100 MHz. In order to compute the field scattered by such a target when probed by means of a line source placed above the interface, one has to evaluate the bound (20). To this end we use (21) for the factor $\|\xi\|$ and the *universal plots* for $\|\mathbf{G}_{22}^{\text{MOD}}\|$. From the tools, it follows that the convergence condition is indeed satisfied as $\|\xi\| \times \|\mathbf{G}_{22}^{\text{MOD}}\| = 0.96 \times 0.97 < 2$. Hence, we can expect that the CS-EB series (17) can be successfully applied to compute the field. This is confirmed by the result shown in Fig. 3(a), where the behavior of the relative error with respect to the actual solution computed via method of moments is reported. For the sake of comparison, the divergent behavior of the Born series is given as well. Note this result could have been foreseen, since the convergence condition for the Born series, computed replacing $\|\xi\|$ with $\|\chi\|$ and $\|\mathbf{G}_{22}^{\text{MOD}}\|$ with $\|\mathbf{G}_{22}\|$, is not fulfilled.

As a second example, let us consider the case of a square target of side 10 m having the characteristics of a water reservoir ($\epsilon = 80$ and $\sigma = 0.2$ [S/m]) buried in a lossy soil ($\epsilon_2 = 4$ and $\sigma_2 = 10^{-2}$ [S/m]). The center of the reservoir is buried at 8 m from the air-soil interface and is probed by a line source working at the frequency of 5 MHz. By again using the above described tools, one gets $\|\xi\| \times \|\mathbf{G}_{22}^{\text{MOD}}\| = 2.51 \times 0.76 < 2$, so that one can expect the convergence of the series iterative scheme, which is indeed confirmed by the behavior of the relative error plotted in Fig. 3(b). For the sake of comparison, in this case we have reported the Born series (that diverges) and the behavior of the over-relaxed CS-EB series which instead allows to

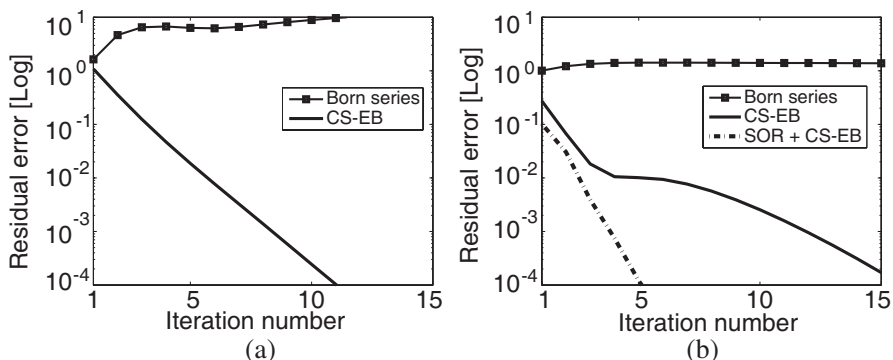


Figure 3. Relative error for the CS-EB and the Born series defined as the square amplitude of the difference between the field at the current iteration and that computed via method of moments. (a) The case of a shallow target of side 0.6 m ($\epsilon = 10, \sigma = 5 \times 10^{-3}$ S/m), buried in a lossy soil ($\epsilon_2 = 4, \sigma_2 = 10^{-2}$ S/m). (b) The case of a water reservoir of side 10 m ($\epsilon = 80, \sigma = 0.2$ S/m) buried in a lossy soil ($\epsilon_2 = 4, \sigma_2 = 10^{-2}$ S/m). For this case, the relative error for the over-relaxed CS-EB series is shown as well.

strongly reduce the number of the terms of the series to be considered for a prescribed accuracy with respect the actual solution.

5. EXPLOITING THE CS-EB MODEL AS A BACKBONE FOR INVERSION APPROACHES

In the framework of the CS-EB model, the inverse problem is formulated through Eq. (13), wherein E_s represents the measured and thus noise affected scattered field data and the modified contrast ξ embeds the electromagnetic characteristic of the unknown scatterers. Then, from the formal analogy with the traditional model, it follows that it is possible to directly exploit all usual solution schemes, such as for instance the modified gradient approach [16, 20], the distorted [5] or the quadratic [13] ones.

On the other hand, a remarkable difference is due to the specific DNL pertaining to the models. As a matter of fact, by again taking advantage of the observations done in Section 3, as well as of our previous studies [17, 19, 23, 25], we can argue that in a wide range of cases $\|\xi \mathbf{G}_{22}^{\text{MOD}}\| < \|\chi \mathbf{G}_{22}\|$, so that, the CS-EB model will be generally characterized by a lower degree of nonlinearity. As recalled, this means that use of the CS-EB model as the backbone of a

reconstruction algorithm based on a local iterative scheme can be expected to be more robust against false solution occurrence (without taking into account additional a priori information or enforcing regularization). Let us remark, that this is not always the case, as examples of interest in practical applications can be found wherein the traditional model has to be preferred to the proposed one [25].

Another important difference that arises when using the CS-EB model in the inversion framework is that extracting the electric parameters from ξ does not appear as immediate as extracting them from the contrast χ . However, once an estimate $\hat{\xi}$ of the auxiliary function has been achieved, such a difficulty is simply tackled by minimizing the functional:

$$\Phi(\chi(r)) = \frac{\|[1 + \hat{\xi}(r)f_{\Omega}(r)]\chi(r) - \hat{\xi}(r)\|_D^2}{\|\hat{\xi}(r)\|^2} \quad (25)$$

which provides, in a straightforward way, the reconstructed contrast $\hat{\chi}$. Interestingly, at this stage possible a priori information about the scatterers can be taken into account.

An interesting feature of inverse scattering problems from buried targets is the decrease of the achievable spatial resolution for increasing depth, according to which the faster spatial variation of the unknown contrast can be retrieved only for shallow targets [12]. Although such an observation has been derived for the traditional formulation, it can be applied to the CS-EB formulation as well, again owing to its analogy with the CS model. Accordingly, in order to take into account this spatial resolution variability in the CS-EB framework, one can adopt a regularization by projection strategy in which the unknown modified contrast is expanded onto a wavelet basis as:

$$\xi(r) = \sum_{n=1}^{N_W} x_n \psi_n(r) \quad (26)$$

so that the actual unknowns of the problem are the N_W wavelet coefficients $x = (x_1, \dots, x_{N_W})$ pertaining to the set of wavelet basis functions $[\psi]_1^{N_W}$, whose number N_W is fixed on the basis of degrees of freedom of the available data [12].

The optimization problem is then cast as the iterative minimization of the functional

$$\begin{aligned} \Phi(\mathbf{x}, J^1, \dots, J^{N_T}) = & \sum_{v=1}^{N_T} \frac{\|J^v - \xi E_{\text{inc}}^v - \xi \mathbf{G}_{22}^{\text{MOD}}(J^v)\|_D^2}{\|E_{\text{inc}}^v\|_D^2} \\ & + \sum_{v=1}^{N_T} \frac{\|E_s^v - \mathbf{G}_{21}(J^v)\|_{\Gamma_R}^2}{\|E_s^v\|_{\Gamma_R}^2} \end{aligned} \quad (27)$$

wherein J^v denotes the contrast source in D corresponding to the v -th transmitter. The details of the iterative scheme can be deduced, with some simple changes, from the expressions given in [14].

As a final remark, note also that, when information on the support of the scatterers is available, either a priori or through suitable preprocessing, the function $f_\Omega(\underline{r})$ in (25) can be evaluated taking advantage of the *optimization* rule given in [23]. Otherwise, $f_\Omega(\underline{r})$ is computed with respect to the whole region under test D , as it is done in the evaluation of the operator $\mathbf{G}_{22}^{\text{MOD}}$.

6. CONCLUSION

In this paper, we have derived a CS-EB formulation for 2D subsurface scattering problems. In several situations, the new scattering model, which is different from the corresponding one obtained in free space owing to the different nature of the Green's functions, allows to reduce the degree of nonlinearity of the scattering problem. Hence, in these cases, it provides a reliable alternative to methods based on the traditional source type integral equation. In particular, we have given tools and (empirical) criteria to evaluate the DNL, so that one can appraise which model is the convenient one to be adopted. Possible future developments include the extension to the 3D geometry (along the lines drawn in [19, 20]) and the derivation of a CS-EB formulation for a non-homogeneous embedding medium.

REFERENCES

1. Chew, W. C., *Waves and Fields in Inhomogeneous Media*, IEEE Press, Piscataway, NJ, 1995.
2. Wang, J. J., *Generalized Moment Methods in Electromagnetics*, Wiley, New York, 1991.
3. Zwamborn, P. and P. M. Van Den Berg, "The three-dimensional weak form of the conjugate gradient FFT method for solving scattering problems," *IEEE Trans. Microw. Theory Tech.*, Vol. 40, No. 9, 1757–1766, 1992.
4. Habashy, T. M., R. W. Groom, and B. R. Spies, "Beyond the born and rytov approximations: A non-linear approach to electromagnetic scattering," *Jour. Geoph. Research*, Vol. 98, 1795–1775, 1993.
5. Cui, T. J., W. C. Chew, and W. Hong, "New approximate formulations for EM scattering by dielectric objects," *IEEE Trans. Antennas Propagat.*, Vol. 52, 684–692, 2004.

6. Christiansen, S., "A preconditioner for the electric field integral equation based on the Calderon formulas," *SIAM J. Numer. Anal.*, Vol. 40, No. 3, 1100–1135, 2002.
7. Ewe, W. B., L. W. Li, Q. Wu, and M. S. Leong, "Preconditioners for adaptive integral methods implementation," *IEEE Trans. Antennas Propagat.*, Vol. 53, No. 7, 2346–2350, 2005.
8. Colton, D. and R. Kress, *Inverse Acoustic and Electromagnetic Scattering Theory*, Springer Verlag, Berlin, Germany, 1992.
9. Van Den Berg, P. M. and A. Abubakar, "Contrast source inversion method: State of the art," *Progress In Electromagnetics Research*, PIER 34, 189–218, 2001.
10. Tijhuis, A. G., K. Belkebir, A. C. S. Litman, and B. P. De Hon, "Theoretical and computational aspects of 2-D inverse profiling," *IEEE Trans. Geosci. Rem. Sensing*, Vol. 39, No. 6, 1316–1330, 2001.
11. Cui, T. J., W. C. Chew, A. A. Aydiner, and S. Chen, "Inverse scattering of two-dimensional dielectric objects buried in a lossy earth using the distorted Born iterative method," *IEEE Trans. Geosci. Rem. Sensing*, Vol. 39, No. 2, 339–346, 2001.
12. Bucci, O. M., L. Crocco, T. Isernia, and V. Pascazio, "Subsurface inverse scattering problems: Quantifying, qualifying, and achieving the available information," *IEEE Trans. Geosci. Rem. Sensing*, Vol. 39, No. 11, 2527–2538, 2001.
13. Leone, G., R. Persico, and R. Solimene, "A quadratic model for electromagnetic subsurface prospecting," *Int. J. Electron. Commun. (AE)*, Vol. 57, 33, 2003.
14. Catapano, I., L. Crocco, and T. Isernia, "A simple two-dimensional inversion technique for imaging homogeneous targets in stratified media," *Radio Science*, Vol. 39, No. 1, 148–161, 2004.
15. Bozza, G., C. Estatico, M. Pastorino, and A. Randazzo, "Application of an inexact-newton method within the second-order born approximation to buried objects," *IEEE Geosci. Rem. Sens. Lett.*, Vol. 4, No. 1, 51–55, 2007.
16. Isernia, T., V. Pascazio, and R. Pierri, "On the local minima in a tomographic imaging technique," *IEEE Trans. Geosci. Rem. Sensing*, Vol. 39, 1596–1607, 2001.
17. Isernia, T., L. Crocco, and M. D'Urso, "New tools and series for scattering problems in lossy media," *IEEE Geosci. Rem. Sens. Lett.*, Vol. 1, No. 4, 327–331, 2004.
18. Catapano, I., L. Crocco, M. D'Urso, and T. Isernia, "A novel effective model for solving 3D inverse scattering problems in lossy

- scenarios," *IEEE Geosci. Rem. Sens. Lett.*, Vol. 3, No. 3, 302–306, 2006.
19. D'Urso, M., I. Catapano, L. Crocco, and T. Isernia, "Effective solution of 3D scattering problems via series expansions: Applicability and a new hybrid scheme," *IEEE Trans. Geosci. Rem. Sensing*, Vol. 45, No. 3, 639–648, 2007.
 20. Van Den Berg, P. M. and R. E. Kleinman, "A contrast source inversion method," *Inverse Problems*, Vol. 13, 1607–1620, 1997.
 21. Bucci, O. M., N. Cardace, L. Crocco, and T. Isernia, "Degree of non-linearity and a new solution procedure in scalar 2-D inverse scattering problems," *J. Opt. Soc. Am. A*, Vol. 18, 1832–1845, 2001.
 22. Crocco, L., M. D'Urso, and T. Isernia, "Testing the contrast source extended born method against real data: The TM case," *Inverse Problems*, Vol. 21, No. 6, S33–S50, 2005.
 23. Catapano, I., L. Crocco, M. D'Urso, and T. Isernia, "On the effect of support estimation and of a new model in 2-D inverse scattering problems," *IEEE Trans. Antennas Propagat.*, Vol. 55, No. 6, 1895–1899, June 2007.
 24. Catapano, I., L. Crocco, M. D'Urso, and T. Isernia, "3D microwave imaging via preliminary support reconstruction: Testing on the Fresnel 2008 database," *Inverse Problems*, Vol. 25, 024002–024025, 2009.
 25. D'Urso, M., T. Isernia, and A. F. Morabito, "On the solution of 2D inverse scattering problems via source type integral equations," *IEEE Trans. Geosci. Rem. Sensing*, in print, 2009.
 26. Kleinman, R. E., G. F. Roach, and P. M. Van Den Berg, "Convergent Born series for large refractive indices," *J. Opt. Soc. Am. A*, Vol. 7, 890–897, 1990.
 27. Yosida, K., *Functional Analysis*, 6th edition, Springer-Verlag, Berlin, Germany, 1980.